

A Note on the Hausdorff Distance between Norm Balls and their Linear Maps

Shadi Haddad^{1*} and Abhishek Halder^{1†}

^{1*}Applied Mathematics, University of California at Santa Cruz,
1156 High Street, Santa Cruz, 95064, California, USA.

*Corresponding author(s). E-mail(s): shhaddad@ucsc.edu;
Contributing authors: ahalder@ucsc.edu;

†These authors contributed equally to this work.

Abstract

We consider the problem of computing the (two-sided) Hausdorff distance between the unit ℓ_{p_1} and ℓ_{p_2} norm balls in finite dimensional Euclidean space for $1 \leq p_1 < p_2 \leq \infty$, and derive a closed-form formula for the same. We also derive a closed-form formula for the Hausdorff distance between the k_1 and k_2 unit D -norm balls, which are certain polyhedral norm balls in d dimensions for $1 \leq k_1 < k_2 \leq d$. When two different ℓ_p norm balls are transformed via a common linear map, we obtain several estimates for the Hausdorff distance between the resulting convex sets. These estimates upper bound the Hausdorff distance or its expectation, depending on whether the linear map is arbitrary or random. We then generalize the developments for the Hausdorff distance between two set-valued integrals obtained by applying a parametric family of linear maps to different ℓ_p unit norm balls, and then taking the Minkowski sums of the resulting sets in a limiting sense. To illustrate an application, we show that the problem of computing the Hausdorff distance between the reach sets of a linear dynamical system with different unit norm ball-valued input uncertainties, reduces to this set-valued integral setting.

Keywords: Hausdorff distance, Convex geometry, Norm balls, Reach set.

1 Introduction

Given compact $\mathcal{X}, \mathcal{Y} \subset \mathbb{R}^d$, the two sided Hausdorff distance δ between them is a mapping $\delta : \mathcal{X} \times \mathcal{Y} \mapsto \mathbb{R}_{\geq 0}$ defined as

$$\delta(\mathcal{X}, \mathcal{Y}) := \max \left\{ \sup_{\mathbf{x} \in \mathcal{X}} \inf_{\mathbf{y} \in \mathcal{Y}} \|\mathbf{x} - \mathbf{y}\|_2, \sup_{\mathbf{y} \in \mathcal{Y}} \inf_{\mathbf{x} \in \mathcal{X}} \|\mathbf{x} - \mathbf{y}\|_2 \right\}, \quad (1)$$

where $\|\cdot\|_2$ is the Euclidean norm with the associated scalar product $\langle \cdot, \cdot \rangle$. Denoting the unit 2 norm ball in \mathbb{R}^d as \mathbb{B}_2^d , an equivalent definition of the Hausdorff distance is

$$\delta(\mathcal{X}, \mathcal{Y}) := \inf \{ \lambda \geq 0 \mid \mathcal{X} \subset \mathcal{Y} \dot{+} \lambda \mathbb{B}_2^d, \mathcal{Y} \subset \mathcal{X} \dot{+} \lambda \mathbb{B}_2^d \}, \quad (2)$$

where $\dot{+}$ denotes the Minkowski sum. As is well-known [1, p. 60-61], $\delta \geq 0$ is a metric. The distance was introduced by Hausdorff in 1914 [2, p. 293ff], and can be considered more generally on the set of nonempty closed and bounded subsets of a metric space $(\mathcal{M}, \text{dist})$ by replacing the Euclidean distance $\|\cdot\|_2$ in (1) with $\text{dist}(\cdot, \cdot)$. The Hausdorff distance and the associated topology, have found widespread applications in mathematical economics [3], stochastic geometry [4], set-valued analysis [5], image processing [6] and pattern recognition [7]. The distance δ has several useful properties with respect to set operations, see e.g., [8, Lemma 2.2], [9, Lemma A2].

The support function $h_{\mathcal{K}}(\cdot)$ of a compact convex set $\mathcal{K} \subset \mathbb{R}^d$, is given by

$$h_{\mathcal{K}}(\mathbf{y}) := \sup_{\mathbf{x} \in \mathcal{K}} \{ \langle \mathbf{y}, \mathbf{x} \rangle \mid \mathbf{y} \in \mathbb{S}^{d-1} \}, \quad (3)$$

where $\langle \cdot, \cdot \rangle$ denotes the standard Euclidean inner product, and \mathbb{S}^{d-1} is the unit sphere in \mathbb{R}^d . The definition (3) can be extended to any closed convex set \mathcal{K} in the sense $h_{\mathcal{K}} = +\infty$ if and only if \mathcal{K} is unbounded [10, Prop. 2.1.3]. Geometrically, $h_{\mathcal{K}}(\mathbf{y})$ gives the signed distance of the supporting hyperplane of \mathcal{K} with outer normal vector \mathbf{y} , measured from the origin. The support function $h_{\mathcal{K}}(\mathbf{y})$ uniquely determines the set \mathcal{K} . Since only the direction of the normal vector \mathbf{y} matters, we restrict the domain of the support function on \mathbb{S}^{d-1} instead of \mathbb{R}^d . Doing so, invites no loss generality because a support function $h_{\mathcal{K}}(\cdot)$ is always positive homogeneous of degree one (see e.g., [10, p. 209]). Furthermore, $h_{\mathcal{K}}(\mathbf{y})$ is a convex function of \mathbf{y} . From (3), we note that for given $\mathbf{T} \in \mathbb{R}^{d' \times d}$ and compact convex $\mathcal{K} \subset \mathbb{R}^d$, the support function of the compact convex set $\mathbf{T}\mathcal{K} \subset \mathbb{R}^{d'}$ is

$$h_{\mathbf{T}\mathcal{K}}(\mathbf{y}) = h_{\mathcal{K}}(\mathbf{T}^\top \mathbf{y}), \quad \mathbf{y} \in \mathbb{S}^{d'-1}. \quad (4)$$

For more details on the support function, we refer the readers to [10, Ch. V].

The two-sided Hausdorff distance (1) between a pair of convex compact sets \mathcal{K}_1 and \mathcal{K}_2 in \mathbb{R}^d can be expressed in terms of their respective support

functions $h_1(\cdot), h_2(\cdot)$ as

$$\delta(\mathcal{K}_1, \mathcal{K}_2) = \sup_{\mathbf{y} \in \mathbb{S}^{d-1}} |h_1(\mathbf{y}) - h_2(\mathbf{y})|, \quad (5)$$

where the absolute value in the objective can be dispensed if one set is included in another¹. Thus, computing δ leads to an optimization problem over all unit vectors $\mathbf{y} \in \mathbb{S}^{d-1}$.

The support function, by definition, is positive homogeneous of degree one. Therefore, the unit sphere constraint $\|\mathbf{y}\|_2 = 1$ in (5) admits a lossless relaxation to the unit ball constraint $\|\mathbf{y}\|_2 \leq 1$. Even so, problem (5) is nonconvex because its objective is nonconvex in general.

In this study, we consider computing (5) for the case when the sets $\mathcal{K}_1, \mathcal{K}_2$ are different unit norm balls and more generally, linear maps of such norm balls in an Euclidean space. This can be viewed as quantifying the conservatism in approximating a norm ball by another in terms of the Hausdorff distance. We show that computing the associated Hausdorff distances lead to optimizing the difference between norms over the unit sphere or ellipsoid. While bounds on the difference of norms over the unit cube have been studied before [11], the optimization problems arising here seem new, and the techniques in [11] do not apply in our setting.

Motivating application: A practical motivation for our study comes from control theory and formal verification literature [12–20]. There, it is of interest to investigate how controlled dynamical systems evolve relative to each other subject to different set-valued input uncertainties. For example, if the controlled dynamical systems model vehicles driving on road, then one practical question is whether the set of states reachable by one vehicle at a specific time, can intersect the other set, possibly resulting in a collision. The different set-valued inputs in the vehicle context, represent respective actuation uncertainties. Then, a natural way to quantify safety or the lack of it, is by computing the distance between such sets in terms of the Hausdorff metric.

In such applications, for computational ease, one often assumes box-valued (i.e., ℓ_∞ norm ball) input uncertainty sets even though the true input uncertainty sets might be ℓ_p norm balls for $0 < p < \infty$. Such computational approximation in the input uncertainty sets lead to over-approximation of the reach sets [19, Sec. III]. Then, quantifying the conservatism in over-approximation amounts to computing the Hausdorff distance between such reach sets. When the controlled dynamical systems are linear, it turns out that the corresponding Hausdorff distance (5) takes the form

$$\sup_{\|\mathbf{y}\|_2=1} \left(\int_0^t \|\mathbf{T}(\tau)\mathbf{y}\|_{q_2} - \|\mathbf{T}(\tau)\mathbf{y}\|_{q_1} \right) d\tau, \quad 1 \leq q_2 < q_1 \leq \infty,$$

which is what we investigate in Sec. 4 in this paper.

¹This is because $\mathcal{K}_1 \subseteq \mathcal{K}_2$ if and only if $h_1(\mathbf{y}) \leq h_2(\mathbf{y})$ for all $\mathbf{y} \in \mathbb{S}^{d-1}$.

We also provide an application Example in Sec. 4, where the different reach sets result from the motion of a satellite subject to ℓ_2 and ℓ_∞ norm ball-valued uncertain input sets. In this application, the input components denote the radial and tangential thrusts, and depending on the actuators installed (e.g., gas jets, reaction wheel), two different scenarios may arise: one where there are hard bounds on the magnitude of the thrust components (i.e., ℓ_∞ norm ball), and another in which there is bounded thrust magnitude (i.e., ℓ_2 norm ball). So from an engineering perspective, it is natural to quantify the Hausdorff distance between the reach sets resulting from two different types of actuation uncertainties.

Related works: There have been several works on designing approximation algorithms for computing the Hausdorff distance between convex polygons [21], curves [22], images [6], meshes [23] or point cloud data [24]; see also [25–29]. There are relatively few [30] known exact formula for the Hausdorff distance between sets. To the best of the authors’ knowledge, analysis of the Hausdorff distance between norm balls and their linear maps as pursued here, did not appear in prior literature.

Contributions: Our specific contributions are as follows.

- We deduce a closed-form formula for the Hausdorff distance between unit ℓ_{p_1} and ℓ_{p_2} norm balls in \mathbb{R}^d for $1 \leq p_1 < p_2 \leq \infty$, i.e., a formula for $\delta(\mathbb{B}_{p_1}^d, \mathbb{B}_{p_2}^d)$. We provide details on the landscape of the corresponding nonconvex optimization objective. We also derive closed-form formula between the k_1 and k_2 unit D -norm balls in \mathbb{R}^d for $1 \leq k_1 < k_2 \leq d$.
- We derive upper bound for Hausdorff distance between the common linear transforms of the ℓ_p and ℓ_q norm balls. This upper bound is a scaled $2 \rightarrow q$ induced operator norm of the linear map, where $1 \leq q \leq \infty$ and the scaling depends on both p and q . We point out a class of linear maps for which the aforesaid closed-form formula for the Hausdorff distance is recovered, thereby broadening the applicability of the formula.
- Bringing together results from the random matrix theory literature, we provide upper bounds for the expected Hausdorff distance when the linear map is random with independent mean-zero entries for two cases: when the entries have magnitude less than unity, and when the entries are standard Gaussian.
- We provide certain generalization of the aforesaid formulation by considering the Hausdorff distance between two set-valued integrals. These integrals represent convex compact sets obtained by applying a parametric family of linear maps to the unit norm balls, and then taking the Minkowski sums of the resulting sets in a suitable limiting sense. We highlight an application for the same in computing the Hausdorff distance between the reach sets of a controlled linear dynamical system with unit norm ball-valued input uncertainties.

The organization is as follows. In Sec. 2, we consider the Hausdorff distance between unit norm balls for two cases: ℓ_p norm balls for different p , and D -norm balls parameterized by different parameter k . We discuss the landscape

of the corresponding nonconvex optimization problem and derive closed-form formula for the Hausdorff distance. Sec. 3 considers the Hausdorff distance between the common linear transformation of different ℓ_p norm balls, and bounds the same when the linear map is either arbitrary or random. In Sec. 4, we consider an integral version of the problem considered in Sec. 3 and illustrate one application in controlled linear dynamical systems with set-valued input uncertainties where this structure appears. These results could be of independent interest.

Notations and preliminaries: Most notations are introduced in situ. We use $\llbracket n \rrbracket := \{1, 2, \dots, n\}$ to denote the set of natural numbers from 1 to n . Boldfaced lowercase and boldfaced uppercase letters are used to denote the vectors and matrices, respectively. The symbol \mathbb{E} denotes the mathematical expectation, $\text{card}(\cdot)$ denotes the cardinality of a set, the superscript \top denotes matrix transpose, and the superscript \dagger denotes the appropriate pseudo-inverse. For a column vector $\mathbf{x} \in \mathbb{R}^d$ whose components are differentiable with respect to (w.r.t.) a scalar parameter t , the symbol $\dot{\mathbf{x}}$ denotes componentwise derivative of \mathbf{x} w.r.t. t . The notation $\lfloor \cdot \rfloor$ stands for the floor function that returns the greatest integer less than or equal to its real argument. The function $\exp(\cdot)$ with matrix argument denotes the matrix exponential. The inequality \succeq is to be understood in Löwner sense; e.g., saying \mathbf{S} is a symmetric positive semidefinite matrix is equivalent to stating $\mathbf{S} \succeq \mathbf{0}$.

For any norm $\|\cdot\|$ in \mathbb{R}^d , its dual norm $(\|\cdot\|)^*$ is defined to be the support function of its unit norm ball, i.e.,

$$(\|\cdot\|)^*(\mathbf{y}) = \sup_{\|\mathbf{x}\| \leq 1} \langle \mathbf{y}, \mathbf{x} \rangle.$$

The notation above emphasizes that the dual norm is a function of the vector \mathbf{y} . For $1 \leq p \leq \infty$, it is well known that the dual of the ℓ_p norm is the ℓ_q norm where q is the Hölder conjugate of p .

For $1 \leq p, q \leq \infty$, matrix $\mathbf{M} \in \mathbb{R}^{m \times n}$ viewed as a linear map $\mathbf{M} : \ell_p(\mathbb{R}^n) \mapsto \ell_q(\mathbb{R}^m)$, has an associated induced operator norm

$$\|\mathbf{M}\|_{p \rightarrow q} := \sup_{\mathbf{x} \neq \mathbf{0}} \frac{\|\mathbf{M}\mathbf{x}\|_q}{\|\mathbf{x}\|_p} = \sup_{\|\mathbf{x}\|_p=1} \|\mathbf{M}\mathbf{x}\|_q, \quad (6)$$

where as usual $\|\mathbf{x}\|_p := (\sum_{i=1}^n |x_i|^p)^{1/p}$, $\|\mathbf{M}\mathbf{x}\|_q := (\sum_{i=1}^m |(\mathbf{M}\mathbf{x})_i|^q)^{1/q}$ for p, q finite, $\|\cdot\|_\infty$ is the sup norm, and $(\mathbf{M}\mathbf{x})_i$ denotes the i th component of the vector $\mathbf{M}\mathbf{x}$. Several special cases of (6) are well known: the case $p = q$ is the standard matrix p norm, the case $p = \infty, q = 1$ is the Grothendieck problem [31, 32] that features prominently in combinatorial optimization, and its generalization $p \in (1, \infty), q = 1$ is the ℓ_p Grothendieck problem [33]. In our development, the operator norm $\|\mathbf{M}\|_{2 \rightarrow q}$ arises where $1 < q \leq \infty$.

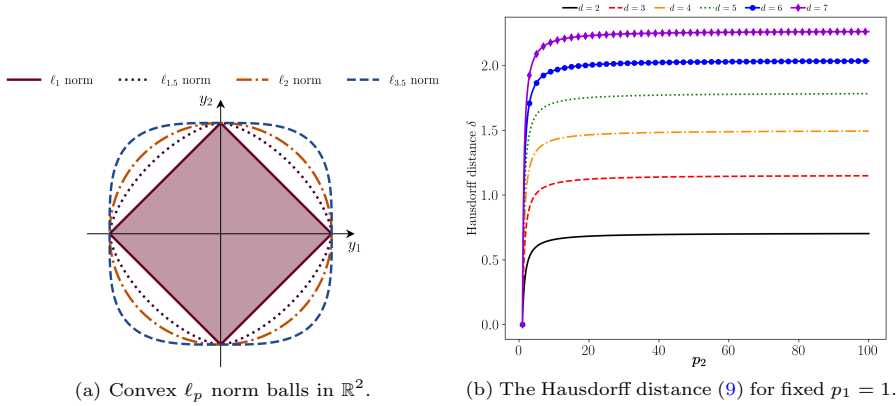


Fig. 1: Understanding the Hausdorff distance δ between the unit ℓ_{p_1} and ℓ_{p_2} norm balls in \mathbb{R}^d , $d \geq 2$, for $1 \leq p_1 < p_2 \leq \infty$.

2 Hausdorff Distance between Unit Norm Balls

We consider the case when in (5), the sets $\mathcal{K}_1 \equiv \mathbb{B}_{p_1}^d$, $\mathcal{K}_2 \equiv \mathbb{B}_{p_2}^d$, the unit ℓ_{p_1} and ℓ_{p_2} norm balls in \mathbb{R}^d , $d \geq 2$, for $1 \leq p_1 < p_2 \leq \infty$. Clearly, the Hausdorff distance $\delta = 0$ for $p_1 = p_2$, and $\delta > 0$ otherwise. Then the corresponding support functions $h_1(\cdot)$, $h_2(\cdot)$ are the respective dual norms, i.e.,

$$h_1(\mathbf{y}) = \|\mathbf{y}\|_{q_1}, \quad h_2(\mathbf{y}) = \|\mathbf{y}\|_{q_2}, \quad \frac{1}{p_1} + \frac{1}{q_1} = 1, \quad \frac{1}{p_2} + \frac{1}{q_2} = 1,$$

for $1 \leq q_2 < q_1 \leq \infty$. By monotonicity of the norm function, we know that $\|\cdot\|_{q_1} \leq \|\cdot\|_{q_2}$. Therefore, the Hausdorff distance (5) in this case becomes

$$\delta(\mathcal{K}_1, \mathcal{K}_2) = \delta(\mathbb{B}_{p_1}^d, \mathbb{B}_{p_2}^d) = \sup_{\|\mathbf{y}\|_2=1} (\|\mathbf{y}\|_{q_2} - \|\mathbf{y}\|_{q_1}) \quad (7)$$

which has a difference of convex (DC) objective. In fact, the objective is non-convex (the difference of convex functions may or may not be convex in general) because it admits multiple global maximizers and minimizers.

The objective in (7) is invariant under the plus-minus sign permutations among the components of the unit vector \mathbf{y} . There are 2^d such permutations feasible in \mathbb{R}^d which implies that the landscape of the objective in (7) has 2^d fold symmetry. In other words, the feasible set is subdivided into 2^d sub-domains as per the sign permutations among the components of \mathbf{y} , and the “sub-landscapes” for these sub-domains are identical.

Since $\|\mathbf{y}\|_{q_1} \leq \|\mathbf{y}\|_{q_2}$ for $1 \leq q_2 < q_1 \leq \infty$, hence $0 \leq \delta$. The *global minimum* value of the objective in (7) is zero, which is achieved by any scaled basis vector, i.e., by $\mathbf{y}^{\min} := \alpha \mathbf{e}_k \in \mathbb{R}^d$ for any $k \in \llbracket d \rrbracket$ and arbitrary $\alpha \in \mathbb{R} \setminus \{0\}$. These \mathbf{y}^{\min} comprise uncountably many global minimizers for (7).

We can compute the *global maximum* value achieved in (7) using the norm inequality

$$\|\cdot\|_{q_2} \leq d^{\frac{1}{q_2} - \frac{1}{q_1}} \|\cdot\|_{q_1}, \quad 1 \leq q_2 < q_1 \leq \infty, \quad (8)$$

which follows from the Hölder's inequality:

$$\sum_{i=1}^d |a_i b_i| \leq \left(\sum_{i=1}^d |a_i|^r \right)^{\frac{1}{r}} \left(\sum_{i=1}^d |b_i|^{\frac{r}{r-1}} \right)^{1-\frac{1}{r}} \quad \mathbf{a}, \mathbf{b} \in \mathbb{R}^d, \quad 1 \leq r \leq \infty,$$

where the exponents r and $\frac{r}{r-1}$ are Hölder conjugates. Applying this inequality with $|a_i| = |x_i|^{q_2}$, $|b_i| = 1$, $r = q_1/q_2 > 1$, results in (8).

In \mathbb{R}^d , the constant $d^{1/q_2 - 1/q_1}$ is sharp because the equality in (8) is achieved by any vector in $\{-1, 1\}^d$. Since (7) has constraint $\|\mathbf{y}\|_2 = 1$, the corresponding global maximum will be achieved by

$$\mathbf{y}^{\max} \in \mathcal{Y}^{\max} := \{\mathbf{u} \in \mathbb{S}^{d-1} \mid \mathbf{u} = \rho \mathbf{v}, \mathbf{v} \in \{-1, 1\}^d, \rho > 0\}.$$

The scalar ρ is determined by the normalization constraint $\|\mathbf{y}^{\max}\|_2 = 1$ as $\rho = 1/\sqrt{d}$. Thus, we obtain

$$\begin{aligned} \delta &= \sup_{\|\mathbf{y}\|_2=1} (\|\mathbf{y}\|_{q_2} - \|\mathbf{y}\|_{q_1}), \quad 1 \leq q_2 < q_1 \leq \infty, \\ &= \left(d^{\frac{1}{q_2} - \frac{1}{q_1}} - 1 \right) \underbrace{\|\mathbf{y}^{\max}\|_{q_1}}_{=\rho d^{\frac{1}{q_1}}}, \end{aligned} \quad (9)$$

where in the last line we substituted $\rho = 1/\sqrt{d}$. The cardinality of \mathcal{Y}^{\max} equals 2^d , i.e., there are 2^d global maximizers $\mathbf{y}^{\max} \in \mathbb{S}^{d-1}$ achieving the value (9).

We summarize the above in the following Proposition.

Proposition 1 *For $1 \leq p_1 < p_2 \leq \infty$, we have*

$$\delta \left(\mathbb{B}_{p_1}^d, \mathbb{B}_{p_2}^d \right) = d^{-\frac{1}{2}} \left(d^{\frac{1}{q_2}} - d^{\frac{1}{q_1}} \right), \quad (10)$$

where q_i denotes the Hölder conjugate of p_i for $i \in \{1, 2\}$.

Remark 1 As the intuition suggests, for a fixed p_1 , larger p_2 results in a larger δ in a given dimension $d \geq 2$; see Fig. 1.

Fig. 2 shows the contour plot of $\|\mathbf{y}\|_1 - \|\mathbf{y}\|_2$ in the spherical coordinates for $d = 3$, i.e., $\mathbf{y} \in \mathbb{S}^2$. As predicted by (9), in this case, there are eight maximizers achieving the global maximum value $\sqrt{3} - 1 \approx 0.7321$. The symmetric sub-landscapes mentioned earlier are also evident in Fig. 2.

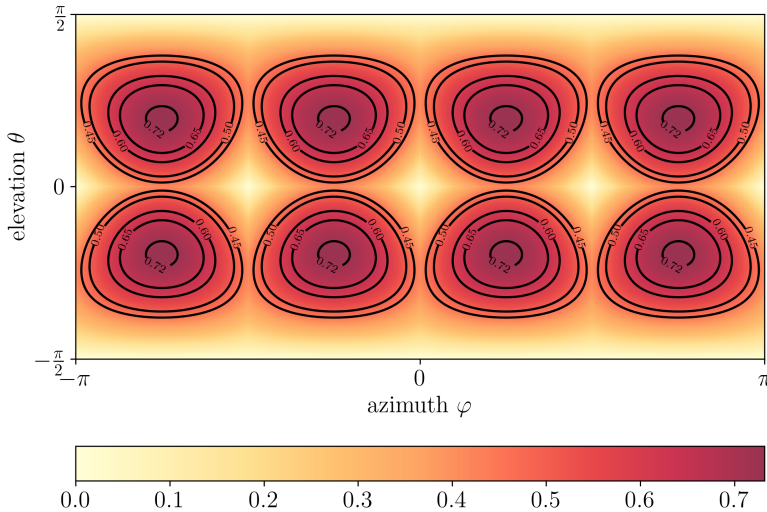


Fig. 2: The landscape of the objective in (7) for $d = 3$, $q_1 = 2$, and $q_2 = 1$.

2.1 Hausdorff Distance between Polyhedral D -Norm Balls

We next show that similar arguments as above can be used to derive the Hausdorff distance between other type of norm balls such as the D -norm balls which are certain polyhedral norm balls. The D -norms and norm balls arise naturally in robust optimization, see e.g., [34, Sec. 2.2], [35]. The D -norm in \mathbb{R}^d is parameterized by k , where $1 \leq k \leq d$, as defined next.

Definition 1 (D -norm) For $1 \leq k \leq d$, the D -norm of $\mathbf{x} \in \mathbb{R}^d$ is

$$\|\mathbf{x}\|_k^D := \max_{\{S \cup \{t\} | S \subseteq \llbracket d \rrbracket, \text{card}(S) \leq k, t \in \llbracket d \rrbracket \setminus S\}} \left\{ \sum_{i \in S} |x_i| + (k - |S|) |x_t| \right\}. \quad (11)$$

For $k = 1$, the norm (11) reduces to the ℓ_∞ norm, i.e., $\|\mathbf{x}\|_1^D = \|\mathbf{x}\|_\infty$. For $k = d$, the norm (11) reduces to the ℓ_1 norm, i.e., $\|\mathbf{x}\|_d^D = \|\mathbf{x}\|_1$. For $1 < k < d$, the norm (11) can be thought of as a polyhedral interpolation between the ℓ_∞ and the ℓ_1 norms. For a plot of the unit D -norm balls in \mathbb{R}^2 , we refer the readers to [34, Fig. 2].

A special case of (11) is when the parameter k is restricted to be a natural number, i.e., $k \in \llbracket d \rrbracket$. Then the D -norm reduces to the so-called k largest magnitude norm, defined next.

Definition 2 (k largest magnitude norm) For $k \in \llbracket d \rrbracket$, the k largest magnitude norm of $\mathbf{x} \in \mathbb{R}^d$ is

$$\|\mathbf{x}\|_{[k]} := |x_{i_1}| + |x_{i_2}| + \dots + |x_{i_k}|, \quad (12)$$

where the inequality $|x_{i_1}| \geq |x_{i_2}| \geq \dots \geq |x_{i_d}|$ denotes the ordering of the magnitudes of the entries in \mathbf{x} .

It is easy to verify that (11) (and thus its special case (12)) is indeed a norm, and its dual norm equals [35, Prop. 2]

$$(\|\cdot\|_k^D)^*(\mathbf{y}) = \max \left\{ \frac{1}{k} \|\mathbf{y}\|_1, \|\mathbf{y}\|_\infty \right\}.$$

For a comparison of the D -norm and its dual with the Euclidean norm, see [35, Prop. 3]. We have the following result.

Proposition 2 (*Hausdorff distance δ between unit D -norm balls*) *Let $1 \leq k_1 < k_2 \leq d$, and let $\mathcal{K}_1, \mathcal{K}_2 \subset \mathbb{R}^d$ denote the unit $\|\cdot\|_{k_1}^D$ and $\|\cdot\|_{k_2}^D$ norm balls in \mathbb{R}^d , i.e., $\mathcal{K}_1 \equiv \mathbb{B}_{\|\cdot\|_{k_1}^D}^d, \mathcal{K}_2 \equiv \mathbb{B}_{\|\cdot\|_{k_2}^D}^d$. Then*

$$\delta(\mathcal{K}_1, \mathcal{K}_2) = \delta \left(\mathbb{B}_{\|\cdot\|_{k_1}^D}^d, \mathbb{B}_{\|\cdot\|_{k_2}^D}^d \right) = \left(\frac{1}{k_1} - \frac{1}{k_2} \right) \sqrt{d}. \quad (13)$$

Proof Let $h_1(\cdot), h_2(\cdot)$ denote the support functions of $\mathcal{K}_1, \mathcal{K}_2$, respectively. Using the definition of dual norm, we have

$$h_1(\mathbf{y}) = \max \left\{ \frac{1}{k_1} \|\mathbf{y}\|_1, \|\mathbf{y}\|_\infty \right\}, \quad h_2(\mathbf{y}) = \max \left\{ \frac{1}{k_2} \|\mathbf{y}\|_1, \|\mathbf{y}\|_\infty \right\}. \quad (14)$$

Recall that δ relates to h_1, h_2 via (5). Since $1 \leq k_1 < k_2 \leq d$, we know that $\frac{1}{k_2} \|\mathbf{y}\|_1 < \frac{1}{k_1} \|\mathbf{y}\|_1$. Depending on the value of $\|\mathbf{y}\|_\infty$, we need to consider three subsets of unit vectors.

Specifically, for the unit vectors \mathbf{y} satisfying $\frac{1}{k_2} \|\mathbf{y}\|_1 < \frac{1}{k_1} \|\mathbf{y}\|_1 \leq \|\mathbf{y}\|_\infty$, we have $h_1(\mathbf{y}) = h_2(\mathbf{y}) = \|\mathbf{y}\|_\infty$ and $h_1(\mathbf{y}) - h_2(\mathbf{y}) = 0$.

On the other hand, for the unit vectors \mathbf{y} satisfying $\|\mathbf{y}\|_\infty \leq \frac{1}{k_2} \|\mathbf{y}\|_1 < \frac{1}{k_1} \|\mathbf{y}\|_1$, we have $h_1(\mathbf{y}) = \frac{1}{k_1} \|\mathbf{y}\|_1, h_2(\mathbf{y}) = \frac{1}{k_2} \|\mathbf{y}\|_1$, hence we obtain that $h_1(\mathbf{y}) - h_2(\mathbf{y}) = (1/k_1 - 1/k_2) \|\mathbf{y}\|_1$, which is always nonnegative.

Finally, for the unit vectors \mathbf{y} satisfying $\frac{1}{k_2} \|\mathbf{y}\|_1 \leq \|\mathbf{y}\|_\infty < \frac{1}{k_1} \|\mathbf{y}\|_1$, we must have $h_1(\mathbf{y}) - h_2(\mathbf{y}) = \frac{1}{k_1} \|\mathbf{y}\|_1 - \|\mathbf{y}\|_\infty < (1/k_1 - 1/k_2) \|\mathbf{y}\|_1$.

Therefore, using (5) we get

$$\delta(\mathcal{K}_1, \mathcal{K}_2) = \left(\frac{1}{k_1} - \frac{1}{k_2} \right) \sup_{\|\mathbf{y}\|_2=1} \|\mathbf{y}\|_1.$$

Using the same arguments as in (9), we obtain $\sup_{\|\mathbf{y}\|_2=1} \|\mathbf{y}\|_1 = \sqrt{d}$, which is achieved by 2^d vectors of the form \mathbf{v}/\sqrt{d} for all $\mathbf{v} \in \{-1, 1\}^d$. This completes the proof. \square

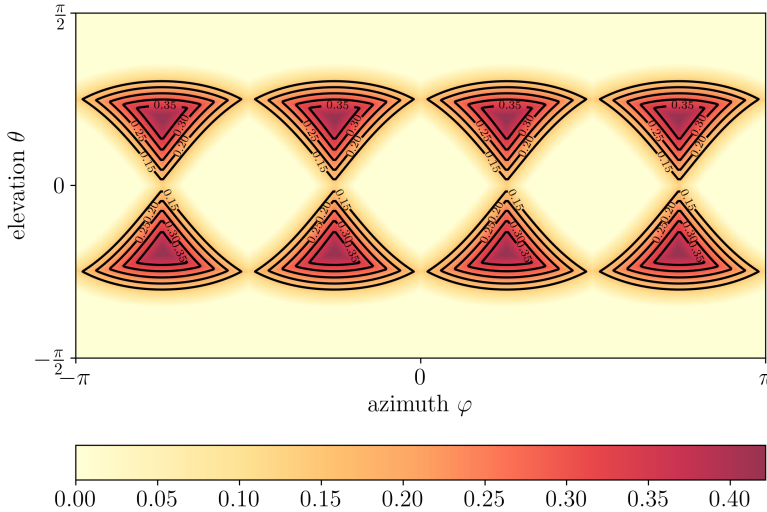


Fig. 3: The landscape of the objective in (5) with h_1, h_2 as in (14) for $d = 3$, $k_1 = 1.7$, and $k_2 = 2.9$.

Fig. 3 shows the landscape of the objective for computing the Hausdorff distance between the unit D -norm balls with $k_1 = 1.7$ and $k_2 = 2.9$ in $d = 3$ dimensions, and as explained in the proof above, there are eight global maximizers given by $\mathbf{v}/\sqrt{3}$ for all $\mathbf{v} \in \{-1, 1\}^3$. In this case, the formula (13) gives $\delta = 120\sqrt{3}/493 \approx 0.421594517055305$ while the direct numerical estimate of δ from the contours yields 0.421577951149235.

3 Composition with a Linear Map

We next consider a generalized version of (7) given by

$$\delta(\mathcal{K}_1, \mathcal{K}_2) = \sup_{\|\mathbf{y}\|_2=1} (\|\mathbf{T}\mathbf{y}\|_{q_2} - \|\mathbf{T}\mathbf{y}\|_{q_1}), \quad 1 \leq q_2 < q_1 \leq \infty, \quad (15)$$

where the matrix $\mathbf{T} \in \mathbb{R}^{m \times d}$, $m \leq d$, has full row rank m . Using (4), we can interpret (15) as follows. As before, let p_1, p_2 denote the Hölder conjugates of q_1, q_2 , respectively. Then (15) computes the Hausdorff distance between two compact convex sets in \mathbb{R}^d obtained as the linear transformations of the m -dimensional ℓ_{p_1} and ℓ_{p_2} unit norm balls via $\mathbf{T}^\top \in \mathbb{R}^{d \times m}$, i.e.,

$$\mathcal{K}_1 \equiv \mathbf{T}^\top \mathbb{B}_{p_1}^d, \quad \mathcal{K}_2 \equiv \mathbf{T}^\top \mathbb{B}_{p_2}^d.$$

Since the right pseudo-inverse $\mathbf{T}^\dagger = \mathbf{T}^\top (\mathbf{T}\mathbf{T}^\top)^{-1}$, one can equivalently view (15) as that of maximizing the difference between the ℓ_{p_1} and ℓ_{p_2} norms over the m -dimensional origin-centered ellipsoid with shape matrix $\mathbf{T}\mathbf{T}^\top$.

As was the case in (7), problem (15) is a DC programming problem with nonconvex objective. However, unlike (7), now there is no obvious symmetry in the objective's landscape that can be leveraged because the number and locations of the local maxima or saddles have sensitive dependence on the matrix parameter \mathbf{T} ; see the first column of Table 1. Thus, directly using off-the-shelf solvers such as [36, 37] or nonconvex search algorithms become difficult for solving (15) in practice as the iterative search may get stuck in a local stationary point.

Remark 2 We can also consider the Hausdorff distance between the common linear transforms of different polyhedral D norm balls discussed earlier. Specifically, if $\mathcal{K}_1, \mathcal{K}_2$ are the unit $\|\cdot\|_{k_1}^D, \|\cdot\|_{k_2}^D$ norm balls for $1 \leq k_1 < k_2 \leq d$, then following (4) and the same steps in the proof of Proposition 2, the Hausdorff distance δ between the sets $\mathbf{T}\mathcal{K}_1, \mathbf{T}\mathcal{K}_2$ equals

$$\delta(\mathbf{T}\mathcal{K}_1, \mathbf{T}\mathcal{K}_2) = \left(\frac{1}{k_1} - \frac{1}{k_2} \right) \underbrace{\sup_{\|\mathbf{y}\|_2=1} \|\mathbf{T}^\top \mathbf{y}\|_1}_{=:\|\mathbf{T}^\top\|_{2 \rightarrow 1}} = \left(\frac{1}{k_1} - \frac{1}{k_2} \right) \|\mathbf{T}\|_{\infty \rightarrow 2}, \quad (16)$$

where the last equality follows from the relation between the induced norm of an operator and that of its adjoint.

3.1 Estimates for Arbitrary \mathbf{T}

We next provide an upper bound for (15) in terms of the operator norm $\|\mathbf{T}\|_{2 \rightarrow q_1}$.

Proposition 3 (Upper bound) *Let $\mathbf{T} \in \mathbb{R}^{m \times d}$. Then for $1 \leq q_2 < q_1 \leq \infty$, we have*

$$\sup_{\|\mathbf{y}\|_2=1} (\|\mathbf{T}\mathbf{y}\|_{q_2} - \|\mathbf{T}\mathbf{y}\|_{q_1}) \leq \left(m^{\frac{1}{q_2} - \frac{1}{q_1}} - 1 \right) \|\mathbf{T}\|_{2 \rightarrow q_1}. \quad (17)$$

Proof Proceeding as in Sec. 2, for $\mathbf{y} \in \mathbb{S}^{d-1}$ we get

$$\begin{aligned} \|\mathbf{T}\mathbf{y}\|_{q_2} &\leq m^{\frac{1}{q_2} - \frac{1}{q_1}} \|\mathbf{T}\mathbf{y}\|_{q_1} \\ \Rightarrow \|\mathbf{T}\mathbf{y}\|_{q_2} - \|\mathbf{T}\mathbf{y}\|_{q_1} &\leq \left(m^{\frac{1}{q_2} - \frac{1}{q_1}} - 1 \right) \|\mathbf{T}\mathbf{y}\|_{q_1} \\ &\leq \left(m^{\frac{1}{q_2} - \frac{1}{q_1}} - 1 \right) \sup_{\|\mathbf{y}\|_2=1} \|\mathbf{T}\mathbf{y}\|_{q_1} = \left(m^{\frac{1}{q_2} - \frac{1}{q_1}} - 1 \right) \|\mathbf{T}\|_{2 \rightarrow q_1} \\ \Rightarrow \sup_{\|\mathbf{y}\|_2=1} (\|\mathbf{T}\mathbf{y}\|_{q_2} - \|\mathbf{T}\mathbf{y}\|_{q_1}) &\leq \left(m^{\frac{1}{q_2} - \frac{1}{q_1}} - 1 \right) \|\mathbf{T}\|_{2 \rightarrow q_1}. \end{aligned}$$

□

Recall that $1 < q_1 \leq \infty$. When $1 \leq q_2 < q_1 \leq 2$, the operator norm $\|\mathbf{T}\|_{2 \rightarrow q_1}$ is, in general, NP hard to compute [38–40] except in the well-known

case $q_1 = 2$ for which $\|\mathbf{T}\|_{2 \rightarrow 2} = \sigma_{\max}(\mathbf{T})$, the maximum singular value of \mathbf{T} . When $1 \leq q_2 \leq 2 < q_1 \leq \infty$, the norm $\|\mathbf{T}\|_{2 \rightarrow q_1}$ is often referred to as hypercontractive [41], and its computation for generic $\mathbf{T} \in \mathbb{R}^{m \times d}$ is relatively less explored (see e.g., [41, 42]) except for the case $q_1 = \infty$ for which $\mathbf{T}_{2 \rightarrow \infty} = \max_{i=1, \dots, m} \|\mathbf{T}(i, :)\|_2$ (maximum ℓ_2 norm of a row). Hypercontractive norms and related inequalities find applications in establishing rapid mixing of random walks as well as several problems of interest in theoretical computer science [41, 43–45].

Table 1 reports our numerical experiments to estimate (15) with $q_1 = 2, q_2 = 1$, for five random realizations of $\mathbf{T} \in \mathbb{R}^{3 \times 3}$, arranged as the rows of Table 1. For visual clarity, the contour plots in the first column of Table 1 depict only four high-magnitude contour levels. These results suggest that the landscape of the nonconvex objective in (15) has sensitive dependence on the mapping \mathbf{T} .

We can say more for specific classes of \mathbf{T} . For example, notice from (17) that if the mapping $\mathbf{T} : \ell_q(\mathbb{R}^d) \mapsto \ell_q(\mathbb{R}^m)$ is an isometry, i.e., $\|\mathbf{T}\mathbf{y}\|_q = \|\mathbf{y}\|_q$, then the upper bound is achieved by any $\mathbf{y} \in \mathbb{R}^d$ such that $\sqrt{d}\mathbf{y} \in \{-1, 1\}^d$ as in Sec. 2, and we recover the exact formula (10). We can characterize these isometric maps as follows.

Proposition 4 (Isometry) Consider a linear mapping given by $\mathbf{T} : \ell_q(\mathbb{R}^d) \mapsto \ell_q(\mathbb{R}^m)$.

(i) (See e.g., [46, Remark 3.1]) For $q = 2$, the mapping $\mathbf{T} \in \mathbb{R}^{m \times d}$ is an isometry if and only if $\mathbf{T}^\top \mathbf{T} = \mathbf{I}_d$, i.e., \mathbf{T} is a column-orthonormal matrix.

(ii) ([46, Thm. 3.2]) For $q \in [1, \infty) \setminus \{2\}$, the mapping $\mathbf{T} \in \mathbb{R}^{m \times d}$ is an isometry if and only if there exists a permutation matrix $\mathbf{P} \in \mathbb{R}^{m \times m}$ such that $\mathbf{P}\mathbf{T} = \text{diag}(\mathbf{r}_1, \mathbf{r}_2, \dots, \mathbf{r}_d)$ and $\|\mathbf{r}_j\|_q = 1$ for all $j \in [d]$. In particular, when $d = m$ and $q \in [1, \infty) \setminus \{2\}$, the mapping \mathbf{T} is isometry if and only if it is a signed permutation matrix [47, 48], i.e., a permutation matrix whose nonzero entries are either all +1 or all -1 or some +1 and the rest -1.

The following is an immediate consequence of this characterization.

Corollary 5 For \mathbf{T} as in Proposition 4, the Hausdorff distance δ in (15) equals (10).

An instance in which $\|\mathbf{T}\|_{2 \rightarrow q_1}$ and hence the bound (17) is efficiently computable, occurs when $\mathbf{T} \in \mathbb{R}^{m \times d}$ is elementwise nonnegative and $1 \leq q_1 < 2$. In this case, the operator norm $\|\mathbf{T}\|_{2 \rightarrow q_1}$ is known [39, Thm. 3.3] to be equal to the optimal value of the following convex optimization problem:

$$\begin{aligned} \text{OPT} &:= \max_{\mathbf{X} \succeq \mathbf{0}} \sqrt{\|\text{dg}(\mathbf{T}\mathbf{X}\mathbf{T}^\top)\|_{\frac{q_1}{2}}} \\ &\text{subject to } \|\text{dg}(\mathbf{X})\|_1 \leq 1, \end{aligned} \quad (18)$$

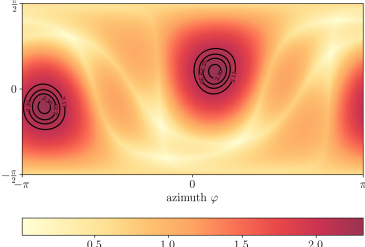
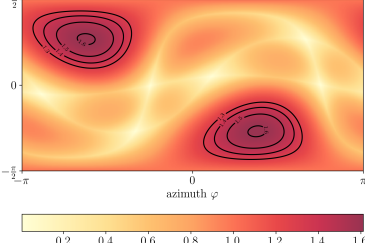
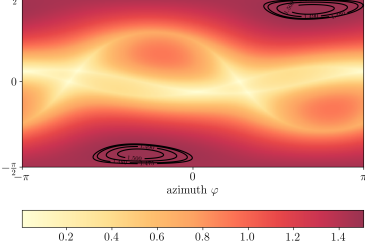
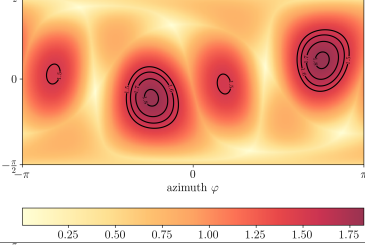
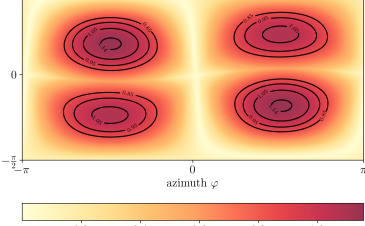
Landscape	Estimated max.	Upper bound (17)
	2.318732079842860	2.384527280099902
	1.611342375325351	1.722680031455154
	1.507938701982408	1.583409927359882
	1.824182821725298	2.157801577048147
	1.154650461995163	1.303457527919837

Table 1: Landscapes of $\|\mathbf{T}\mathbf{y}\|_{q_2} - \|\mathbf{T}\mathbf{y}\|_{q_1}$ for $q_1 = 2, q_2 = 1, \mathbf{y} \in \mathbb{S}^2$ in spherical coordinates for five randomly generated $\mathbf{T} \in \mathbb{R}^{3 \times 3}$ with independent standard Gaussian entries. The middle column reports the numerically estimated global maxima from the respective contour data, i.e., the estimated Hausdorff distance (15). The last column shows the corresponding bounds (17).

where $\text{dg}(\cdot)$ takes a square matrix as its argument and returns the vector comprising of the diagonal entries of that matrix. To see why problem (18) is convex, notice that $\mathbf{X} \succeq \mathbf{0}$ has unique (principal) square root, so $\mathbf{T}\mathbf{X}\mathbf{T}^\top = \mathbf{T}\mathbf{X}^{\frac{1}{2}}\left(\mathbf{T}\mathbf{X}^{\frac{1}{2}}\right)^\top \succeq \mathbf{0}$ which implies $\text{dg}(\mathbf{T}\mathbf{X}\mathbf{T}^\top)$ has nonnegative entries. Consequently, the objective in (18) is concave for $1 \leq q_1 < 2$. The non-empty feasible set $\{\mathbf{X} \in \mathbb{R}^{d \times d} \mid \mathbf{X} \succeq \mathbf{0}, \|\text{dg}(\mathbf{X})\|_1 = \sum_{i=1}^d X_{ii} \leq 1\}$ is the intersection of the positive semidefinite cone with a linear inequality, hence convex (in fact a spectrahedron).

Then, the right hand side of (17) equals $\left(m^{\frac{1}{q_2} - \frac{1}{q_1}} - 1\right) \times \text{OPT}$. For example, when

$$q_1 = 1.5, \quad q_2 = 1, \quad \mathbf{T} = \begin{bmatrix} 2 & 6 & 0 \\ 5 & 0 & 1 \end{bmatrix}, \quad (19)$$

a numerical solution of (18) via `cvx` [49] gives $\text{OPT} \approx 7.425702405524379$. As in Table 1, a direct numerical search over the nonconvex landscape (Fig. 4) for this example returns the estimated Hausdorff distance $\approx 1.888517738190415$ while using the numerically computed OPT, we find the upper bound (17) $\approx 1.930096365450782$.

Remark 3 We clarify here that for (18) to be used in the upper bound (17), the range of q_1 is $1 < q_1 < 2$. That $\|\mathbf{T}\|_{2 \rightarrow q_1}$ equals to (18) holds also for the case $q_1 = 1$. Indeed, this implies we can compute (16) for elementwise nonnegative \mathbf{T} by computing $\|\mathbf{T}^\top\|_{2 \rightarrow 1}$ via convex optimization.

3.2 Estimates for Random \mathbf{T}

For random linear maps $\mathbf{T} : \ell_q(\mathbb{R}^d) \mapsto \ell_q(\mathbb{R}^m)$, it is possible to bound the expected Hausdorff distance (15). We collect two such results in the following proposition.

Proposition 6 (Bound for the expected Hausdorff distance)

Let $2 \leq q_1 < \infty$.

(i) Let $\mathbf{T} = (\theta_{ij})_{i,j=1}^{m,d}$ have independent (not necessarily identically distributed) mean-zero entries with $|\theta_{ij}| \leq 1$ for all index pair (i, j) . Then the Hausdorff distance (15) satisfies

$$\mathbb{E} \delta \leq \left(m^{\frac{1}{q_2} - \frac{1}{q_1}} - 1\right) C_{q_1} \max\{m^{\frac{1}{q_1}}, \sqrt{d}\} \quad (20)$$

where the pre-factor C_{q_1} depends only on q_1 .

(ii) Let $\mathbf{T} = (\theta_{ij})_{i,j=1}^{m,d}$ have independent standard Gaussian entries. Then the Hausdorff distance (15) satisfies

$$\mathbb{E} \delta \leq C \left(m^{\frac{1}{q_2} - \frac{1}{q_1}} - 1\right) 2^{5/q_1} (\log m)^{1/q_1} \left(\gamma_2 + \gamma_{q_1} \mathbb{E} \max_{i,j} |\theta_{ij}|\right) + 2^{1/q_1} \gamma_{q_1} \quad (21)$$

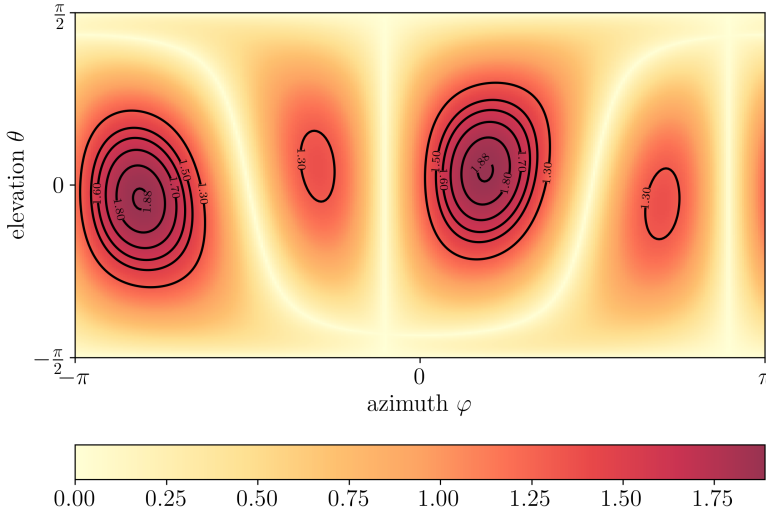


Fig. 4: The landscape of the objective in (15) depicted in spherical coordinates for the problem data given in (19).

where $C > 0$ is a constant, and $\gamma_r := (\mathbb{E}|X|^r)^{1/r}$, $r \geq 1$, is the L_r norm of a standard Gaussian random variable X . In particular, $\gamma_r \asymp \sqrt{r}$, i.e., there exist positive constants c_1, c_2 such that $c_1\sqrt{r} \leq \gamma_r \leq c_2\sqrt{r}$ for all $r \geq 1$.

Proof (i) Following [50, Thm. 1], we bound the expected operator norm as $\mathbb{E}\|\mathbf{T}\|_{2 \rightarrow q_1} \leq C_{q_1} \max\{m^{1/q_1}, \sqrt{d}\}$. Combining this with (17), the result follows.

(ii) The expected $2 \rightarrow q_1$ operator norm bound, in this case, follows from specializing more general bound² given in [51, Thm. 1.1]. Specifically, we get

$$\mathbb{E}\|\mathbf{T}\|_{2 \rightarrow q_1} \leq C 2^{5/q_1} (\log m)^{1/q_1} \left(\gamma_2 + \gamma_{q_1} \mathbb{E} \max_{i,j} |a_{ij}| \right) + 2^{1/q_1} \gamma_{q_1}, \quad (22)$$

where $C, \gamma_2, \gamma_{q_1}$ are as in the statement. Combining (22) with (17), we obtain (21). \square

4 Integral Version and Application

We now consider a further generalization of (15) given by

$$\delta(\mathcal{K}_1, \mathcal{K}_2) = \sup_{\|\mathbf{y}\|_2=1} \int_0^t (\|\mathbf{T}(\tau)\mathbf{y}\|_{q_2} - \|\mathbf{T}(\tau)\mathbf{y}\|_{q_1}) \, d\tau, \quad 1 \leq q_2 < q_1 \leq \infty, \quad (23)$$

where for each $\tau \in [0, t]$, the matrix $\mathbf{T}(\tau) \in \mathbb{R}^{m \times d}$, $m \leq d$, is smooth in τ and has full row rank m .

²The operator norm bound in [51, Thm. 1.1] is more general on two counts. First, the operator norm considered there is $p^* \rightarrow q$ where $1 \leq p^* \leq 2 \leq q \leq \infty$. Second, the result therein allows nonuniform deterministic scaling of the standard Gaussian entries of \mathbf{T} .

As before, let p_1, p_2 denote the Hölder conjugates of q_1, q_2 , respectively. We can interpret (23) as computing the Hausdorff distance between two compact convex sets in \mathbb{R}^d obtained by first taking linear transformations of the m -dimensional p_1 and p_2 unit norm balls via $\mathbf{T}^\top(\tau) \in \mathbb{R}^{d \times m}$ for fixed $\tau \in [0, t]$, and then taking respective Minkowski sums for varying τ and finally passing to the limit. In particular, if we let $\mathcal{P}_i := \{\mathbf{v} \in \mathbb{R}^m \mid \|\mathbf{v}\|_{p_i} \leq 1\}$ for $i \in \{1, 2\}$, then (23) computes the Hausdorff distance between the d dimensional compact convex sets

$$\mathcal{K}_1 \equiv \int_0^t \mathbf{T}^\top(\tau) \mathcal{P}_1 d\tau := \lim_{\Delta \downarrow 0} \sum_{i=0}^{\lfloor t/\Delta \rfloor} \Delta \mathbf{T}^\top(i\Delta) \mathcal{P}_1, \quad (24a)$$

$$\mathcal{K}_2 \equiv \int_0^t \mathbf{T}^\top(\tau) \mathcal{P}_2 d\tau := \lim_{\Delta \downarrow 0} \sum_{i=0}^{\lfloor t/\Delta \rfloor} \Delta \mathbf{T}^\top(i\Delta) \mathcal{P}_2, \quad (24b)$$

i.e., the sets under consideration are set-valued Aumann integrals [52] and the symbol \sum denotes the Minkowski sum. That the sets in (24) are convex is a consequence of the Lyapunov convexity theorem [53, 54].

Notice that in this case, (17) directly yields

$$\begin{aligned} \delta(\mathcal{K}_1, \mathcal{K}_2) &\leq \int_0^t \sup_{\|\mathbf{y}\|_2=1} (\|\mathbf{T}(\tau)\mathbf{y}\|_{q_2} - \|\mathbf{T}(\tau)\mathbf{y}\|_{q_1}) d\tau \\ &\leq \left(m^{\frac{1}{q_2} - \frac{1}{q_1}} - 1\right) \int_0^t \|\mathbf{T}(\tau)\|_{2 \rightarrow q_1} d\tau. \end{aligned} \quad (25)$$

A different way to deduce (25) is to utilize the definitions (24), and then combine the Hausdorff distance property in [8, Lemma 2.2(ii)] with a limiting argument. This gives

$$\delta\left(\int_0^t \mathbf{T}^\top(\tau) \mathcal{P}_1 d\tau, \int_0^t \mathbf{T}^\top(\tau) \mathcal{P}_2 d\tau\right) \leq \int_0^t \delta(\mathbf{T}^\top(\tau) \mathcal{P}_1, \mathbf{T}^\top(\tau) \mathcal{P}_2) d\tau. \quad (26)$$

For a fixed $\tau \in [0, t]$, the integrand in the right hand side of (26) is precisely (15), hence using Proposition 3 we again arrive at (25).

As a motivating application, consider two controlled linear dynamical agents with identical dynamics given by the ordinary differential equation

$$\dot{\mathbf{x}}^i(t) = \mathbf{A}(t)\mathbf{x}^i(t) + \mathbf{B}(t)\mathbf{u}^i(t), \quad i \in \{1, 2\}, \quad (27)$$

where $\mathbf{x}^i(t) \in \mathbb{R}^d$ is the state and $\mathbf{u}^i(t) \in \mathbb{R}^m$ is the control input for the i th agent at time t . Suppose that the system matrices $\mathbf{A}(t), \mathbf{B}(t)$ are smooth measurable functions of t , and that the initial conditions for the two agents have the same compact convex set valued uncertainty, i.e., $\mathbf{x}^i(t=0) \in$ compact convex $\mathcal{X}_0 \subset \mathbb{R}^d$. Furthermore, suppose that the input uncertainty sets for the

two systems are given by different unit norm balls

$$\mathcal{U}^i := \{\mathbf{u}^i(\tau) \in \mathbb{R}^m \mid \|\mathbf{u}^i(\tau)\|_{p_i} \leq 1 \text{ for all } \tau \in [0, t]\}, \quad i \in \{1, 2\}, \quad (28)$$

such that $1 \leq p_1 < p_2 \leq \infty$. Given these set-valued uncertainties, the “reach sets” \mathcal{X}_t^i , $i \in \{1, 2\}$, are defined as the respective set of states each agent may reach at a given time $t > 0$. Specifically, for $i \in \{1, 2\}$, and \mathcal{U}^i given by (28), the reach sets are

$$\begin{aligned} \mathcal{X}_t^i := & \bigcup_{\text{measurable } \mathbf{u}^i(\cdot) \in \mathcal{U}^i} \{\mathbf{x}^i(t) \in \mathbb{R}^d \mid \dot{\mathbf{x}}^i(t) = \mathbf{A}(t)\mathbf{x}^i(t) + \mathbf{B}(t)\mathbf{u}^i(t), \quad i \in \{1, 2\}, \\ & \mathbf{x}^i(t=0) \in \text{compact convex } \mathcal{X}_0, \quad \mathbf{u}^i(\tau) \in \mathcal{U}^i \text{ for all } 0 \leq \tau \leq t\}. \end{aligned} \quad (29)$$

As such, there exists a vast literature [12–20] on reach sets and their numerical approximations. In practice, these sets are of interest because their separation or intersection often imply safety or the lack of it. It is natural to quantify the distance between reach sets or their approximations in terms of the Hausdorff distance [55–57], and in our context, this amounts to estimating $\delta(\mathcal{X}_t^1, \mathcal{X}_t^2)$.

Since $1 \leq p_1 < p_2 \leq \infty$, we have the norm ball inclusion $\mathcal{U}^1 \subset \mathcal{U}^2$, and consequently $\mathcal{X}_t^1 \subset \mathcal{X}_t^2$. We next show that $\delta(\mathcal{X}_t^1, \mathcal{X}_t^2)$ is exactly of the form (23).

Theorem 7 (Hausdorff distance between linear systems’ reach sets with norm ball input uncertainty) Consider the reach sets (29) with input set valued uncertainty (28). For $\tau \leq t$, let $\Phi(t, \tau)$ be the state transition matrix (see e.g., [58, Ch. 1.3]) associated with (27). Denote the Hölder conjugate of p_1 as q_1 , and that of p_2 as q_2 , i.e., $1/p_1 + 1/q_1 = 1$ and $1/p_2 + 1/q_2 = 1$. Then $1 \leq q_2 < q_1 \leq \infty$, and the Hausdorff distance

$$\delta(\mathcal{X}_t^1, \mathcal{X}_t^2) = \sup_{\|\mathbf{y}\|_2=1} \int_0^t \left(\|(\Phi(t, \tau)\mathbf{B}(\tau))^\top \mathbf{y}\|_{q_2} - \|(\Phi(t, \tau)\mathbf{B}(\tau))^\top \mathbf{y}\|_{q_1} \right) d\tau. \quad (30)$$

Proof We have

$$\mathcal{X}_t^i = \Phi(t, 0)\mathcal{X}_0 \dot{+} \int_0^t \Phi(t, \tau)\mathbf{B}(\tau)\mathcal{U}^i d\tau, \quad i \in \{1, 2\}, \quad (31)$$

where $\dot{+}$ denotes the Minkowski sum and the second summand in (31) is a set-valued Aumann integral.

Since the support function is distributive over the Minkowski sum, following [59, Prop. 1] and (3), from (31) we find that

$$h_i(\mathbf{y}) := h_{\mathcal{X}_t^i}(\mathbf{y}) = \left(\sup_{\mathbf{x}_0 \in \mathcal{X}_0} \langle \mathbf{y}, \Phi(t, 0)\mathbf{x}_0 \rangle \right) + \int_0^t \sup_{\mathbf{u}^i(\tau) \in \mathcal{U}^i} \langle \mathbf{y}, \Phi(t, \tau)\mathbf{B}(\tau)\mathbf{u}^i(\tau) \rangle d\tau, \quad (32)$$

wherein $i \in \{1, 2\}$ and the sets \mathcal{U}^i are given by (28). Next, we follow the same arguments as in [60, Thm. 1] to simplify (32) as

$$h_i(\mathbf{y}) = \left(\sup_{\mathbf{x}_0 \in \mathcal{X}_0} \langle \mathbf{y}, \Phi(t, 0)\mathbf{x}_0 \rangle \right) + \int_0^t \| (\Phi(t, \tau)\mathbf{B}(\tau))^\top \mathbf{y} \|_{q_i} d\tau, \quad (33)$$

where q_i is the Hölder conjugate of p_i . Then (5) together with (33) yield (30). \square

Corollary 8 *Using the same notations of Theorem 7, we have*

$$\delta(\mathcal{X}_t^1, \mathcal{X}_t^2) \leq \left(m^{\frac{1}{q_2} - \frac{1}{q_1}} - 1 \right) \int_0^t \| \Phi(t, \tau)\mathbf{B}(\tau) \|_{p_1 \rightarrow 2} d\tau. \quad (34)$$

Proof From (25), we obtain the estimate

$$\delta(\mathcal{X}_t^1, \mathcal{X}_t^2) \leq \left(m^{\frac{1}{q_2} - \frac{1}{q_1}} - 1 \right) \int_0^t \| (\Phi(t, \tau)\mathbf{B}(\tau))^\top \|_{2 \rightarrow q_1} d\tau. \quad (35)$$

Recall that the norm of a linear operator is related to the norm of its adjoint via

$$\| (\cdot)^\top \|_{\alpha \rightarrow \beta} = \| \cdot \|_{\beta^* \rightarrow \alpha^*},$$

where α^*, β^* are the Hölder conjugates of α, β , respectively. Using this fact in (35) completes the proof. \square

Remark 4 In the special case of a linear time invariant dynamics, the matrices \mathbf{A}, \mathbf{B} in (27) are constants and $\Phi(t, \tau) = \exp((t - \tau)\mathbf{A})$. In that case, Theorem 7 and Corollary 8 apply with these additional simplifications.

Remark 5 As t increases, we expect the bound (25) to become more conservative. Likewise, the gap between (30) and (34) is expected to increase with t .

Example. Consider the linearized equation of motion of a satellite [58, p. 14–15] of the form (27) with four states, two control inputs, and constant system matrices

$$\mathbf{A}(t) \equiv \begin{bmatrix} 0 & 1 & 0 & 0 \\ 3\omega^2 & 0 & 0 & 2\omega \\ 0 & 0 & 0 & 1 \\ 0 & -2\omega & 0 & 0 \end{bmatrix}, \quad \mathbf{B}(t) \equiv \begin{bmatrix} 0 & 0 \\ 1 & 0 \\ 0 & 0 \\ 0 & 1 \end{bmatrix}, \quad (36)$$

for some fixed parameter ω . The input components denote the radial and tangential thrusts, respectively. We consider two cases: the inputs have set-valued uncertainty of the form (28) with $p_1 = 2$ (unit Euclidean norm-bounded

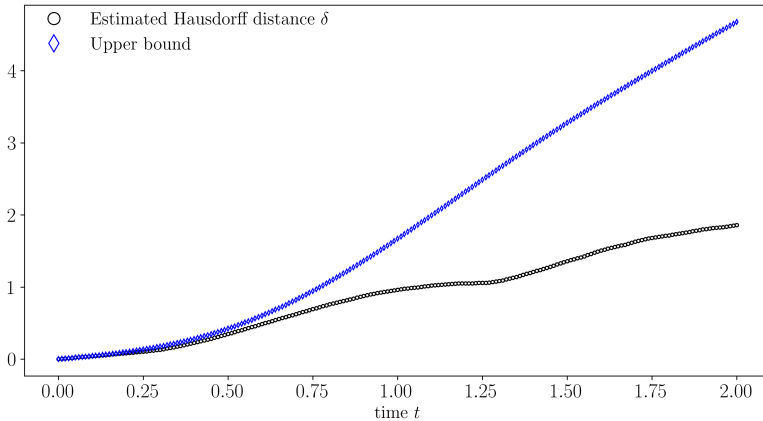


Fig. 5: The numerically estimated Hausdorff distance (30) and the upper bound (34) for the four state, two input linear system given in (36).

thrust) and with $p_2 = \infty$ (unit box-valued thrust). We have [58, p. 41]

$$\Phi(t, \tau)B = \begin{bmatrix} \frac{\sin(\omega(t - \tau))}{\omega} & \frac{2(1 - \cos(\omega(t - \tau)))}{\omega} \\ \cos(\omega(t - \tau)) & 2 \sin(\omega(t - \tau)) \\ -\frac{2(1 - \cos(\omega(t - \tau)))}{\omega} & \frac{-3\omega(t - \tau) + 4 \sin(\omega(t - \tau))}{\omega} \\ -2 \sin(\omega(t - \tau)) & -3 + 4 \sin(\omega(t - \tau)) \end{bmatrix},$$

for $0 \leq \tau < t$, and the integrand in the right hand side of (34) equals to the maximum singular value of the above matrix. For $\omega = 3$ and $t \in [0, 2]$, Fig. 5 shows the time evolution of the numerically estimated Hausdorff distance (30) and the upper bound (34) between the reach sets given by (29) with the same compact convex initial set $\mathcal{X}_0 \subset \mathbb{R}^4$, i.e., between \mathcal{X}_t^1 and \mathcal{X}_t^2 resulting from the unit $p_1 = 2$ and $p_2 = \infty$ norm ball input sets, respectively.

5 Conclusions

In this work, we studied the Hausdorff distance between two different norm balls in an Euclidean space and derived closed-form formula for the same. In d dimensions, we provide results for the ℓ_p norm balls parameterized by p where $1 \leq p \leq \infty$, as well as for the polyhedral D -norm balls parameterized by k where $1 \leq k \leq d$. We then investigated a more general setting: the Hausdorff distance between two convex sets obtained by transforming two different ℓ_p norm balls via a given linear map. In this setting, while we do not know a general closed-form formula for an arbitrary linear map, we provide upper

bounds for the Hausdorff distance or its expected value depending on whether the linear map is arbitrary or random. Our results make connections with the literature on hypercontractive operator norms, and on the norms of random linear maps. We then focus on a further generalization: the Hausdorff distance between two set-valued integrals obtained by applying a parametric family of linear maps to the unit ℓ_p norm balls, and then taking the Minkowski sums of the resulting sets in a limiting sense. As an illustrative application, we show that the problem of computing the Hausdorff distance between the reach sets of a linear time-varying dynamical system with different unit ℓ_p norm ball-valued input uncertainties, leads to this set-valued integral setting.

We envisage several directions of future work. It is natural to further explore the qualitative properties of the nonconvex landscape (15), and to design efficient algorithms in computing the Hausdorff distance for the same. It should also be of interest to pursue a systems-control theoretic interpretation of (30) and (34) in terms of functionals of the associated controllability Gramian.

Supplementary information. ‘Not applicable’.

Availability of data and materials. The datasets that support our results in this study are available from the authors on request.

References

- [1] Schneider, R.: Convex Bodies: the Brunn–Minkowski Theory (ser. Encyclopedia of Mathematics and Its Applications) vol. 151. Cambridge university press, (2014)
- [2] Hausdorff, F.: Grundzüge der Mengenlehre vol. 7. von Veit, (1914)
- [3] Hildenbrand, W.: Core and equilibria of a large economy.(psme-5). In: Core and Equilibria of a Large Economy.(PSME-5). Princeton university press, (2015)
- [4] Stoyan, D., Kendall, W.S., Chiu, S.N., Mecke, J.: Stochastic Geometry and Its Applications. John Wiley & Sons, (2013)
- [5] Serra, J.: Hausdorff distances and interpolations. Computational Imaging and Vision **12**, 107–114 (1998)
- [6] Huttenlocher, D.P., Klanderman, G.A., Rucklidge, W.J.: Comparing images using the Hausdorff distance. IEEE Transactions on pattern analysis and machine intelligence **15**(9), 850–863 (1993)
- [7] Jesorsky, O., Kirchberg, K.J., Frischholz, R.W.: Robust face detection using the Hausdorff distance. In: International Conference on Audio-and Video-based Biometric Person Authentication, pp. 90–95 (2001). Springer

- [8] De Blasi, F.: On the differentiability of multifunctions. *Pacific Journal of Mathematics* **66**(1), 67–81 (1976)
- [9] Serry, M., Reissig, G.: Overapproximating reachable tubes of linear time-varying systems. *IEEE Transactions on Automatic Control* **67**(1), 443–450 (2021)
- [10] Hiriart-Urruty, J.-B., Lemaréchal, C.: *Convex Analysis and Minimization Algorithms I: Fundamentals* vol. 305. Springer, (2013)
- [11] Shisha, O., Mond, B.: Differences of means. *Bulletin of the American Mathematical Society* **73**(3), 328–333 (1967)
- [12] Pecsvaradi, T., Narendra, K.S.: Reachable sets for linear dynamical systems. *Information and control* **19**(4), 319–344 (1971)
- [13] Witsenhausen, H.: A remark on reachable sets of linear systems. *IEEE Transactions on Automatic Control* **17**(4), 547–547 (1972)
- [14] Chutinan, A., Krogh, B.H.: Verification of polyhedral-invariant hybrid automata using polygonal flow pipe approximations. In: *Hybrid Systems: Computation and Control: Second International Workshop, HSCC’99 Berg en Dal, The Netherlands, March 29–31, 1999 Proceedings 2*, pp. 76–90 (1999). Springer
- [15] Kurzhanski, A., Vályi, I.: *Ellipsoidal Calculus for Estimation and Control*. Springer, (1997)
- [16] Varaiya, P.: Reach set computation using optimal control. *Verification of Digital and Hybrid Systems*, 323–331 (2000)
- [17] Le Guernic, C., Girard, A.: Reachability analysis of linear systems using support functions. *Nonlinear Analysis: Hybrid Systems* **4**(2), 250–262 (2010)
- [18] Althoff, M., Frehse, G., Girard, A.: Set propagation techniques for reachability analysis. *Annual Review of Control, Robotics, and Autonomous Systems* **4**, 369–395 (2021)
- [19] Haddad, S., Halder, A.: The curious case of integrator reach sets, part i: Basic theory. *Transactions on Automatic Control* (2023)
- [20] Haddad, S., Halder, A.: Anytime ellipsoidal over-approximation of forward reach sets of uncertain linear systems. In: *Proceedings of the Workshop on Computation-Aware Algorithmic Design for Cyber-Physical Systems*, pp. 20–25 (2021)
- [21] Atallah, M.J.: A linear time algorithm for the Hausdorff distance between

- convex polygons. *Information Processing Letters* **17**(4), 207–209 (1983)
- [22] Belogay, E., Cabrelli, C., Molter, U., Shonkwiler, R.: Calculating the Hausdorff distance between curves. *Information Processing Letters* **64**(1) (1997)
- [23] Aspert, N., Santa-Cruz, D., Ebrahimi, T.: Mesh: Measuring errors between surfaces using the Hausdorff distance. In: *Proceedings. IEEE International Conference on Multimedia and Expo*, vol. 1, pp. 705–708 (2002). IEEE
- [24] Taha, A.A., Hanbury, A.: An efficient algorithm for calculating the exact Hausdorff distance. *IEEE transactions on pattern analysis and machine intelligence* **37**(11), 2153–2163 (2015)
- [25] Goffin, J.-L., Hoffman, A.J.: On the relationship between the Hausdorff distance and matrix distances of ellipsoids. *Linear algebra and its applications* **52**, 301–313 (1983)
- [26] Alt, H., Behrends, B., Blömer, J.: Approximate matching of polygonal shapes. *Annals of Mathematics and Artificial Intelligence* **13**(3), 251–265 (1995)
- [27] Alt, H., Braß, P., Godau, M., Knauer, C., Wenk, C.: Computing the hausdorff distance of geometric patterns and shapes. *Discrete and Computational Geometry: The Goodman-Pollack Festschrift*, 65–76 (2003)
- [28] König, S.: Computational aspects of the Hausdorff distance in unbounded dimension. *Journal of Computational Geometry* **5**(1), 250–274 (2014)
- [29] Jungeblut, P., Kleist, L., Miltzow, T.: The complexity of the Hausdorff distance. *arXiv preprint arXiv:2112.04343* (2021)
- [30] Marošević, T.: The Hausdorff distance between some sets of points. *Mathematical Communications* **23**(2), 247–257 (2018)
- [31] Grothendieck, A.: *Résumé de la Théorie Métrique des Produits Tensoriels topologiques*. Soc. de Matemática de São Paulo, (1956)
- [32] Alon, N., Naor, A.: Approximating the cut-norm via Grothendieck’s inequality. In: *Proceedings of the Thirty-sixth Annual ACM Symposium on Theory of Computing*, pp. 72–80 (2004)
- [33] Kindler, G., Naor, A., Schechtman, G.: The UGC hardness threshold of the L_p Grothendieck problem. *Mathematics of Operations Research* **35**(2), 267–283 (2010)
- [34] Rahal, S., Li, Z.: Norm induced polyhedral uncertainty sets for robust

- linear optimization. *Optimization and Engineering*, 1–37 (2021)
- [35] Bertsimas, D., Pachamanova, D., Sim, M.: Robust linear optimization under general norms. *Operations Research Letters* **32**(6), 510–516 (2004)
- [36] DCCP Python package, GitHub repository. URL: <https://github.com/cvxgrp/dccp>
- [37] Shen, X., Diamond, S., Gu, Y., Boyd, S.: Disciplined convex-concave programming. In: 2016 IEEE 55th Conference on Decision and Control (CDC), pp. 1009–1014 (2016). IEEE
- [38] Hendrickx, J.M., Olshevsky, A.: Matrix p -norms are NP-hard to approximate if $p \neq 1, 2, \infty$. *SIAM Journal on Matrix Analysis and Applications* **31**(5), 2802–2812 (2010)
- [39] Steinberg, D.: Computation of matrix norms with applications to robust optimization. Research thesis, Technion-Israel University of Technology **2** (2005)
- [40] Bhaskara, A., Vijayaraghavan, A.: Approximating matrix p -norms. In: Proceedings of the Twenty-second Annual ACM-SIAM Symposium on Discrete Algorithms, pp. 497–511 (2011). SIAM
- [41] Barak, B., Brandao, F.G., Harrow, A.W., Kelner, J., Steurer, D., Zhou, Y.: Hypercontractivity, sum-of-squares proofs, and their applications. In: Proceedings of the Forty-fourth Annual ACM Symposium on Theory of Computing, pp. 307–326 (2012)
- [42] Bhattiprolu, V., Ghosh, M., Guruswami, V., Lee, E., Tulsiani, M.: Approximability of $p \rightarrow q$ matrix norms: generalized Krivine rounding and hypercontractive hardness. In: Proceedings of the Thirtieth Annual ACM-SIAM Symposium on Discrete Algorithms, pp. 1358–1368 (2019). SIAM
- [43] Gross, L.: Logarithmic Sobolev inequalities. *American Journal of Mathematics* **97**(4), 1061–1083 (1975)
- [44] Saloff-Coste, L.: Lectures on finite Markov chains. Lectures on probability theory and statistics (Saint-Flour, 1996), 301–413. *Lecture Notes in Math* **1665** (1997)
- [45] Biswal, P.: Hypercontractivity and its applications. arXiv preprint arXiv:1101.2913 (2011)
- [46] Wang, C., Zheng, D.-S., Chen, G.-L., Zhao, S.-Q.: Structures of p -isometric matrices and rectangular matrices with minimum p -norm

- condition number. *Linear algebra and its applications* **184**, 261–278 (1993)
- [47] Li, C.-K., So, W.: Isometries of ℓ_p norm. *The American mathematical monthly* **101**(5), 452–453 (1994)
- [48] Glueck, J.: What are the matrices preserving the ℓ^1 -norm? MathOverflow. URL: <https://mathoverflow.net/q/288084> (version: 2017-12-09). <https://mathoverflow.net/q/288084>
- [49] Grant, M., Boyd, S.: CVX: Matlab Software for Disciplined Convex Programming, version 2.1. <http://cvxr.com/cvx> (2014)
- [50] Bennett, G., Goodman, V., Newman, C.: Norms of random matrices. *Pacific Journal of Mathematics* **59**(2), 359–365 (1975)
- [51] Guédon, O., Hinrichs, A., Litvak, A.E., Prochno, J.: On the expectation of operator norms of random matrices. In: *Geometric Aspects of Functional Analysis*, pp. 151–162. Springer, (2017)
- [52] Aumann, R.J.: Integrals of set-valued functions. *Journal of Mathematical Analysis and Applications* **12**(1), 1–12 (1965)
- [53] Liapounoff, A.: Sur les fonctions-vecteurs completement additives. *Izvestiya Rossiiskoi Akademii Nauk. Seriya Matematicheskaya* **4**(6), 465–478 (1940)
- [54] Halmos, P.R.: The range of a vector measure. *Bulletin of the American Mathematical Society* **54**(4), 416–421 (1948)
- [55] Guseinov, K.G., Ozer, O., Akyar, E., Ushakov, V.: The approximation of reachable sets of control systems with integral constraint on controls. *Nonlinear Differential Equations and Applications NoDEA* **14**(1), 57–73 (2007)
- [56] Dueri, D., Raković, S.V., Açikmeşe, B.: Consistently improving approximations for constrained controllability and reachability. In: *2016 European Control Conference (ECC)*, pp. 1623–1629 (2016). IEEE
- [57] Halder, A.: Smallest ellipsoid containing p -sum of ellipsoids with application to reachability analysis. *IEEE Transactions on Automatic Control* **66**(6), 2512–2525 (2020)
- [58] Brockett, R.W.: *Finite Dimensional Linear Systems*. John Wiley & Sons, Inc., (1970)
- [59] Haddad, S., Halder, A.: The convex geometry of integrator reach sets. In: *2020 American Control Conference (ACC)*, pp. 4466–4471 (2020). IEEE

- [60] Haddad, S., Halder, A.: Certifying the intersection of reach sets of integrator agents with set-valued input uncertainties. *IEEE Control Systems Letters* **6**, 2852–2857 (2022)